



# B cells migrate into remote brain areas and support neurogenesis and functional recovery after focal stroke in mice

Sterling B. Ortega<sup>a,b,c,1</sup>, Vanessa O. Torres<sup>b,c,1</sup>, Sarah E. Latchney<sup>d,e</sup>, Cody W. Whooley<sup>d</sup>, Ibrahim Z. Noorbhai<sup>b,c</sup>, Katie Poinssatte<sup>b,c</sup>, Uma M. Selvaraj<sup>b,c</sup>, Monica A. Benson<sup>b,c</sup>, Anouk J. M. Meeuwissen<sup>b,c</sup>, Erik J. Plautz<sup>b,c</sup>, Xiangmei Kong<sup>b,c</sup>, Denise M. Ramirez<sup>b,c</sup>, Apoorva D. Ajay<sup>b,c</sup>, Julian P. Meeks<sup>b,c,f</sup>, Mark P. Goldberg<sup>b,c</sup>, Nancy L. Monson<sup>b,c</sup>, Amelia J. Eisch<sup>d,g,h</sup>, and Ann M. Stowe<sup>b,c,i,2</sup>

<sup>a</sup>Department of Pathology, University of Iowa, Iowa City, IA 52242; <sup>b</sup>Department of Neurology and Neurotherapeutics, UT Southwestern Medical Center, Dallas, TX 75390; <sup>c</sup>Peter O'Donnell Jr. Brain Institute, UT Southwestern Medical Center, Dallas, TX 75390; <sup>d</sup>Department of Psychiatry, UT Southwestern Medical Center, Dallas, TX 75390; <sup>e</sup>Department of Biology, St. Mary's College of Maryland, St. Mary's City, MD 20686; <sup>f</sup>Department of Neuroscience, UT Southwestern Medical Center, Dallas, TX 75390; <sup>g</sup>Department of Neuroscience, Perelman School of Medicine, University of Pennsylvania, Philadelphia, PA 19104; <sup>h</sup>Department of Anesthesiology and Critical Care, Children's Hospital of Philadelphia, Philadelphia, PA 19104; and <sup>i</sup>Department of Neurology, University of Kentucky, Lexington, KY 40506

Edited by Lawrence Steinman, Stanford University School of Medicine, Stanford, CA, and approved January 16, 2020 (received for review August 1, 2019)

**Lymphocytes infiltrate the stroke core and penumbra and often exacerbate cellular injury. B cells, however, are lymphocytes that do not contribute to acute pathology but can support recovery. B cell adoptive transfer to mice reduced infarct volumes 3 and 7 d after transient middle cerebral artery occlusion (tMCAo), independent of changing immune populations in recipient mice. Testing a direct neurotrophic effect, B cells cocultured with mixed cortical cells protected neurons and maintained dendritic arborization after oxygen-glucose deprivation. Whole-brain volumetric serial two-photon tomography (STPT) and a custom-developed image analysis pipeline visualized and quantified poststroke B cell diapedesis throughout the brain, including remote areas supporting functional recovery. Stroke induced significant bilateral B cell diapedesis into remote brain regions regulating motor and cognitive functions and neurogenesis (e.g., dentate gyrus, hypothalamus, olfactory areas, cerebellum) in the whole-brain datasets. To confirm a mechanistic role for B cells in functional recovery, rituximab was given to human CD20<sup>+</sup> (hCD20<sup>+</sup>) transgenic mice to continuously deplete hCD20<sup>+</sup>-expressing B cells following tMCAo. These mice experienced delayed motor recovery, impaired spatial memory, and increased anxiety through 8 wk poststroke compared to wild type (WT) littermates also receiving rituximab. B cell depletion reduced stroke-induced hippocampal neurogenesis and cell survival. Thus, B cell diapedesis occurred in areas remote to the infarct that mediated motor and cognitive recovery. Understanding the role of B cells in neuronal health and disease-based plasticity is critical for developing effective immune-based therapies for protection against diseases that involve recruitment of peripheral immune cells into the injured brain.**

B lymphocytes | focal stroke | serial two-photon tomography | adaptive immunity | neurogenesis

**S**troke leads to central nervous system (CNS) damage, which results in functional deficits (1) and is exacerbated by an inflammatory immune response derived from both the innate and adaptive immune systems (2). Mechanistic studies using murine stroke models show a significant infiltration of innate immune cells, including monocytes, macrophages, and neutrophils, predominantly in the area of ischemic injury (i.e., infarct, periinfarct regions) (3). The role of the adaptive immune system is also pivotal to stroke recovery, as it can both exacerbate and ameliorate long-term neuropathology, depending on the lymphocyte population, location, and timing of activation (4–10). Location and timing are particularly relevant, as recovery of lost function in stroke patients depends on functional plasticity in areas outside of the infarct (i.e., remote cortices) to subsume lost function (11).

Neurons in remote cortical areas that are interconnected to the infarct up-regulate growth factors and plasticity-related genes after stroke (12, 13), but it is unknown if neuroinflammation is concomitant with remote genetic and proteomic responses to ischemic injury and subsequent reorganization.

B cells, critical effector cells for antibody production and antigen presentation, are one adaptive immune cell subset with the capacity to also produce neurotrophins to support neuronal survival and plasticity (14–16). Prior work found that the loss of B cells increases stroke-induced infarct volumes, functional deficits, and mortality in immunodeficient  $\mu\text{MT}^{-/-}$  mice, which lack B cells (17). Polyclonal activated and nonactivated B cell

## Significance

**Neuroinflammation occurs immediately after stroke onset in the ischemic infarct, but whether neuroinflammation occurs in remote regions supporting plasticity and functional recovery remains unknown. We used advanced imaging to quantify whole-brain diapedesis of B cells, an immune cell capable of producing neurotrophins. We identify bilateral B cell diapedesis into remote regions, outside of the injury, that support motor and cognitive recovery in young male mice. Poststroke depletion of B cells confirms a positive role in neurogenesis, neuronal survival, and recovery of motor coordination, spatial learning, and anxiety. More than 80% of stroke survivors have long-term disability uniquely affected by age and lifestyle factors. Thus, identifying beneficial neuroinflammation during long-term recovery increases the opportunity of therapeutic interventions to support functional recovery.**

Author contributions: S.B.O., S.E.L., C.W.W., K.P., M.P.G., N.L.M., A.J.E., and A.M.S. designed research; S.B.O., V.O.T., S.E.L., C.W.W., I.Z.N., K.P., U.M.S., M.A.B., A.J.M.M., E.J.P., X.K., D.M.R., A.D.A., J.P.M., M.P.G., A.J.E., and A.M.S. performed research; N.L.M. contributed new reagents/analytic tools; S.B.O., V.O.T., S.E.L., C.W.W., D.M.R., A.D.A., J.P.M., and A.M.S. analyzed data; and S.B.O., V.O.T., S.E.L., C.W.W., N.L.M., A.J.E., and A.M.S. wrote the paper.

The authors declare no competing interest.

This article is a PNAS Direct Submission.

This open access article is distributed under [Creative Commons Attribution-NonCommercial-NoDerivatives License 4.0 \(CC BY-NC-ND\)](https://creativecommons.org/licenses/by-nc-nd/4.0/).

Data deposition: All raw data have been uploaded to Harvard Dataverse, <https://doi.org/10.7910/DVN/RFGT4S>.

<sup>1</sup>S.B.O. and V.O.T. contributed equally to this work.

<sup>2</sup>To whom correspondence may be addressed. Email: [ann.stowe@uky.edu](mailto:ann.stowe@uky.edu).

This article contains supporting information online at <https://www.pnas.org/lookup/suppl/doi:10.1073/pnas.1913292117/-DCSupplemental>.

First published February 12, 2020.

transfer into syngeneic mice also ameliorates stroke pathology and functional deficits within the first 96 h after stroke via interleukin (IL)-10-mediated up-regulation (9, 10). Reconstitution of Rag<sup>-/-</sup> (i.e., B- and T cell-knockout) mice with B cells does not exacerbate infarct volume, confirming a nonpathological role in acute stroke (18, 19). Others confirmed a nonpathological role for B cells after stroke in several other strains (20). However, additional studies do not extend the neuroprotective and/or nonpathological role beyond 4 d after stroke onset, with the only investigation into the long-term role of B cells in stroke recovery finding that B cells contribute to cognitive decline weeks after stroke in multiple strains of mice across various stroke models (21). These data, coupled with human data associating self-reactive antibodies with cognitive decline (8), underscore the importance of additional studies to clarify the contribution of B cells to poststroke injury and repair. This includes the importance of timing, location, and function of B cells recruited into the injured brain in defining the role in either injury or repair.

The goal of this series of experiments is to elucidate the endogenous role of B cells, including localization of B cell diapedesis after stroke using advanced volumetric imaging strategies (e.g., serial two-photon tomography), and the behavioral relevance of B cells using refined neurological motor and cognitive assessments. In this work, we show that poststroke B cell repletion reduces neuropathology via an IL-10-dependent mechanism that is independent of immune modulation. Second, we show that B cells exert a direct neuroprotective effect on neurons and preserve neuronal dendritic arborization following oxygen-glucose deprivation *in vitro*. We find that B cells diapedese bilaterally into remote areas of the brain that associate with long-term motor and cognitive function following a transient middle cerebral artery occlusion (tMCAo), while long-term depletion of B cells after stroke exacerbates motor and cognitive deficits and reduces poststroke neurogenesis. In summary, we show that B cells play a prominent role in stroke recovery beyond the first 4 d after stroke by directly protecting neurons and promoting recovery within the injured and reorganizing brain.

## Results

**B Cells Use IL-10 to Reduce Stroke-Induced Neuropathology.** Previously published studies found that B cells exhibit conflicting roles in stroke recovery dependent on the state of activation: acute *in vitro* activation benefits (i.e., 1 to 4 d) versus long-term *in vivo* activation detriments (i.e., months) (10, 21). Furthermore, the use of antibody-mediated B cell depletion in wild type and transgenic mice revealed no change in the neuropathology or functional deficits at the acute phase of stroke (days 1 and 3 post induction) (20). Thus, to further dissect the role of B cells in subacute to long-term stroke recovery, we investigated the endogenous function of B cells by adoptive transfer of naïve, wild type B cells into stroke-induced recipient mice, measuring neuropathology and motor coordination at time points up to 2 wk following stroke induction. We purified unstimulated B cells from naïve mice and injected them *i.v.* into recipient mice 7 h after stroke onset (60-min tMCAo; Fig. 1A). On all mice, successful tMCAo induction was qualified as a 20% reduction for 60 min followed by reperfusion to at least 50% of baseline (pretMCAo induction) cerebral blood flow. We measured motor function using rotarod (days 2, 6, and 14 poststroke), forearm strength (force grip), neuropathology via T2-weighted MRI (days 3 and 7), and cytotoxicity via standard histology (day 15). Relative to PBS controls, B cell recipients exhibited reduced infarctions identified by serial MRI at both 3 d ( $P < 0.01$ ) and 7 d ( $P < 0.05$ ; Fig. 1B and C) post tMCAo. Interestingly, the rotarod and force grip assays did not detect differences between the two cohorts, even though all groups initiated acute deficits confirming similar degree of initial stroke-induced neuropathology (SI Appendix, Fig. S1A and B). We sought to determine if naïve B cells, without *in vitro* activation, caused reduced infarct volumes via an IL-10-mediated mechanism. Adoptive transfer of wild type B cells from naïve mice reduced infarct volume, and this protection was lost with IL-10-deficient B cells (Fig. 1D). As protection was absent in both IL-10-deficient (Fig. 1D) and “preconditioned” (22) B cells (SI Appendix, Fig. S1B and C), these data show that naïve B cells provide an endogenous neuroprotective function (22). In contrast to other studies (9),

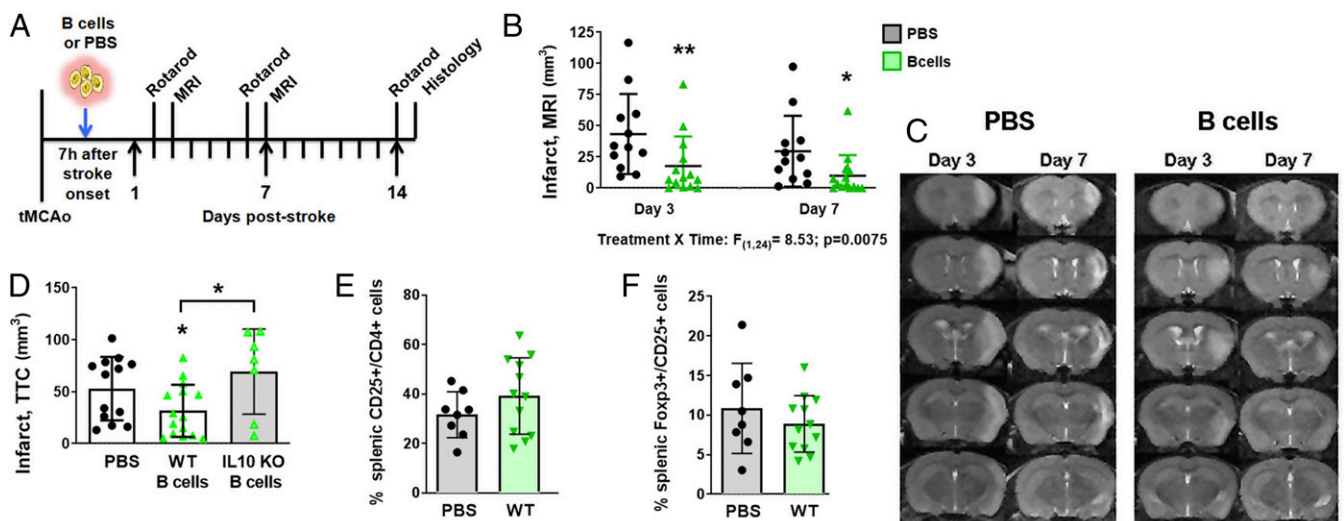


**Fig. 1.** B cell adoptive transfer reduces infarct volumes via IL-10 but independently of immunomodulation. (A) Experimental timeline for B cell adoptive transfer 7 h after tMCAo. (B) Infarct volumes quantified from (C) serial MR images show that naïve B cells (green upward triangles) significantly decrease infarct volumes 3 and 7 d poststroke as compared to PBS control (black circles). (D) B cells isolated from wild type (WT) B6 mice (solid green triangles, white bar) and IL-10 KO mice (open green triangles, gray bar) show that only WT B cells reduced infarct volumes 3 d after tMCAo compared to PBS controls (black circles; determined by one-way ANOVA). (E) WT B cell treatment did not differentially activate CD4<sup>+</sup>CD25<sup>+</sup> T cells in the spleen, nor did they (F) induce a regulatory T cell population in the spleen. Significance determined by two-way repeated-measure ANOVA or Student's *t* test (\* $P < 0.05$ , \*\* $P < 0.01$  vs. PBS control unless indicated by bracket).

protection by naïve B cells was indicated neither by peripheral suppression of activated CD4<sup>+</sup>CD25<sup>+</sup> T cells (Fig. 1E), nor by the induction of splenic regulatory T cell population (Fig. 1F). Together with prior studies showing no induction of regulatory T cells in the CNS by B cell adoptive transfer (10), our data suggest a previously unreported and distinct mechanism employed by the adoptive transfer of naïve B cells during stroke recovery.

**B Cells Directly Promote Neuronal Viability and Dendritic Arborization In Vitro.** One regulatory immune cell-independent mechanism of poststroke neuroprotection that could be induced by B cells is a direct neurotrophic effect of B cells on neurons at risk for cell death (14). Using an in vitro approach to determine a direct role in neuronal protection, mixed cortical cells were subjected to 2 h of oxygen-glucose deprivation (OGD) followed immediately by addition of naïve B cells to the culture for 4 d (Fig. 2A and B). In the mixed cortical culture condition without B cells, OGD caused loss of microtubule-associated protein (MAP2)<sup>+</sup> neurons ( $P < 0.001$ ) and loss of arborization ( $P < 0.01$ ; Fig. 2C

and D). Addition of naïve B cells to cortical cells (0.1:1.0 ratio) reduced both neuronal death ( $P < 0.05$ ) and loss of dendritic arborization ( $P < 0.05$ ). In the absence of ischemic injury, the addition of naïve B cells increased the number of surviving MAP2<sup>+</sup> neurons ( $P < 0.05$ ; Fig. 2C) and increased dendritic arborization ( $P < 0.05$ , 0.1:1.0 ratio;  $P < 0.01$ , 1:1; Fig. 2D) compared to cultures without B cells. Replication of these experiments with naïve IL-10-deficient B cells showed no dose-response effect on neuronal cell loss either with or without OGD (Fig. 2E). In contrast, IL-10-deficient B cells still preserved dendritic arborization after OGD, albeit at a higher concentration ( $P < 0.05$ ; Fig. 2F and *SI Appendix*, Fig. S2). Increased dendritic arborization also occurred in the absence of OGD with IL-10-deficient B cells ( $P < 0.05$ ), suggesting that IL-10 is a redundant mechanism that supports maintenance of mature neurons with dendrites. In summary, these data confirm the capability of naïve B cells for direct neuronal protection in vitro by an IL-10 mechanism within the context of neuronal ischemic injury.

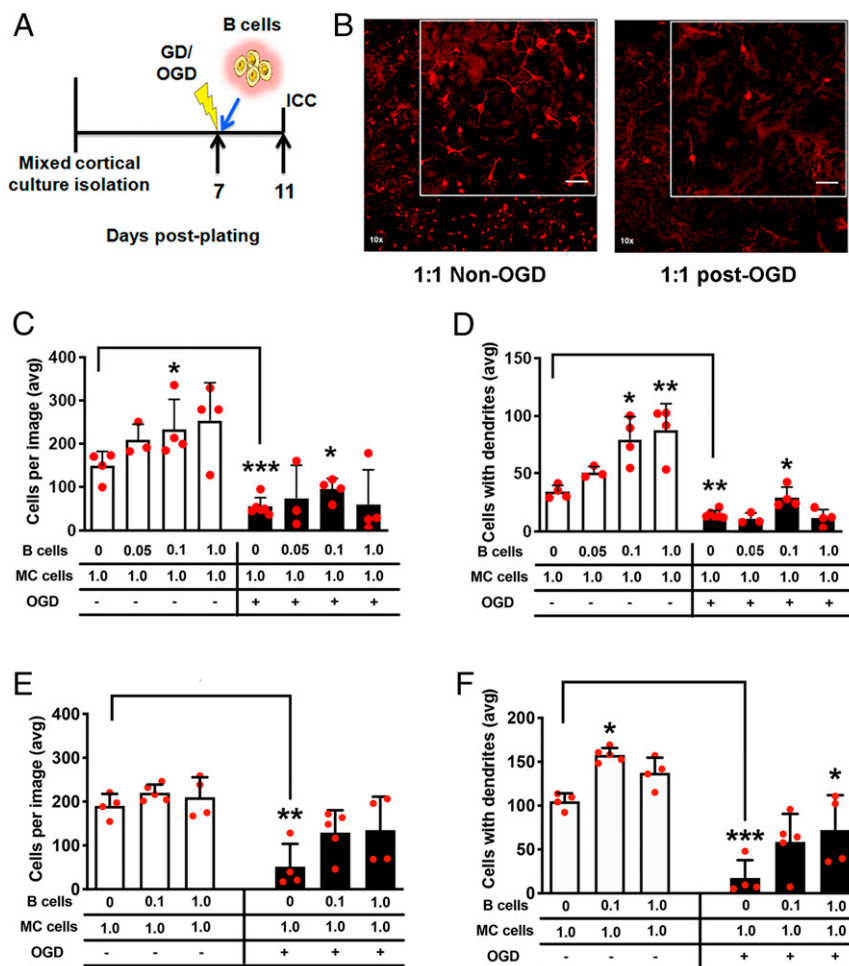


**Fig. 2.** B cells induce a neurotrophic effect in mixed cortical cultures. (A) Experimental timeline for the placement of naïve B cells on culture after oxygen-glucose deprivation (OGD) and prior to immunocytochemistry (ICC). (B) Images at 10 $\times$  of microtubule-associated protein (MAP2)<sup>+</sup> neurons (red) for treatment (txn) groups; higher-magnification image is also shown (*inset*). (Scale bar, 50  $\mu$ m.) (C) Increasing ratio of B cells to mixed cortical (MC) cells increased the number of MAP2<sup>+</sup> neurons, as well as (D) the number of MAP2<sup>+</sup> neurons with dendrites, in the non-OGD experiments. OGD decreased overall numbers, with only a 0.1:1.0 B cell:mixed cortical cell ratio preserving neuronal survival and dendritic arborization. (E and F) Experiments were replicated with IL-10-deficient B cells (images shown in *SI Appendix*, Fig. S2). IL-10-deficient B cells (E) did not preserve cell survival after OGD, but (F) a 1:1 ratio did preserve dendritic arborization after OGD. Replicate, independent experiments (each with interexperimental replicates) are shown by red circles for total  $n$ . Nonparametric one-way ANOVA (Kruskal–Wallis) determined within-group significance, and  $t$  test was used for untreated non-OGD:OGD comparisons. Data graphed as mean  $\pm$  SD, and significance determined by nonparametric one-way ANOVA or Student's  $t$  test (\* $P < 0.05$ , \*\* $P < 0.01$ , \*\*\* $P < 0.001$  vs. untreated control unless otherwise indicated by brackets).

**B Cells Are Present within the Parenchyma of the Poststroke Brain.** At the whole-brain level, B cells are an abundant leukocyte population within the stroke-injured brain 48 h after stroke onset (22, 23). In fact, the cortical and subcortical brain vascular endothelium exhibits an up-regulation of CXCL13, a B cell homing chemokine (22). Recent advances in volumetric whole-brain imaging methods including serial two-photon tomography (STPT) have enabled automated, unbiased methods to visualize and computationally detect signals of interest, including fluorescently labeled cell populations as well as neuronal substructures in the entire brain (24–26). We established a custom pipeline including STPT, supervised machine learning-based pixel classification, and image registration to visualize and quantify adoptively transferred immune cells labeled with the fluorophore e450 throughout the whole mouse brain. We verified this methodology to accurately quantify labeled CD8<sup>+</sup> T cell diapedesis into the whole brain after tMCAo in Poinatte et al., 2019 (27). The output of our machine learning-based pixel classification step is visualized as a probability map of pixels automatically detected by the trained algorithm as B cells (Fig. 3A) (28). The brighter the area in the probability map, the more likely the trained algorithm identified the fluorescence as a B cell.

To quantify whole brain neuroinflammation, we used two cohorts of mice: (i) B cell-depleted recipient hCD20<sup>+</sup> mice or wild type (WT) hCD20<sup>-</sup> B cell donor littermate controls, with all

recipient mice receiving rituximab prior to tMCAo to target hCD20<sup>+</sup> B cells for depletion (29) (Fig. 3B); and (ii) B cell-sufficient C57BL/6 mice with unaltered B cell populations. In order to account for endogenous poststroke autofluorescence secondary to ischemic injury and cell death, we included PBS recipient cohorts. STPT detected signal from fluorescent e450<sup>+</sup> donor hCD20<sup>-</sup> B cells in both the ipsilesional and contralesional hemispheres (Fig. 3C) of B cell-depleted recipient mice ( $P < 0.05$  for both hemispheres vs. PBS; Fig. 3D). We also observed bilateral e450<sup>+</sup> B cell signal in the B cell-sufficient cohort, albeit with larger group variation (Fig. 3E). B cell recipients in both cohorts of mice exhibited e450<sup>+</sup> B cells identified by flow cytometry in both the cervical lymph nodes and spleen 4 d after tMCAo (SI Appendix, Fig. S3), confirming the presence of live B cells following adoptive transfer. The surprising increase of B cells in the contralesional hemisphere indicates that B cell diapedesis is not only localized to infarct and periinfarct areas with high cytokine and chemokine up-regulation, but there is also an active recruitment from the periphery in brain regions remote from the ischemic core.

**Adoptively Transferred B Cells Localize to CNS Motor Nuclei and Areas of Neurogenesis.** We previously observed B cell infiltration into the brain following stroke (22, 30). Now, understanding that B cells could exert in vitro neuroprotection (Fig. 2), we wanted to

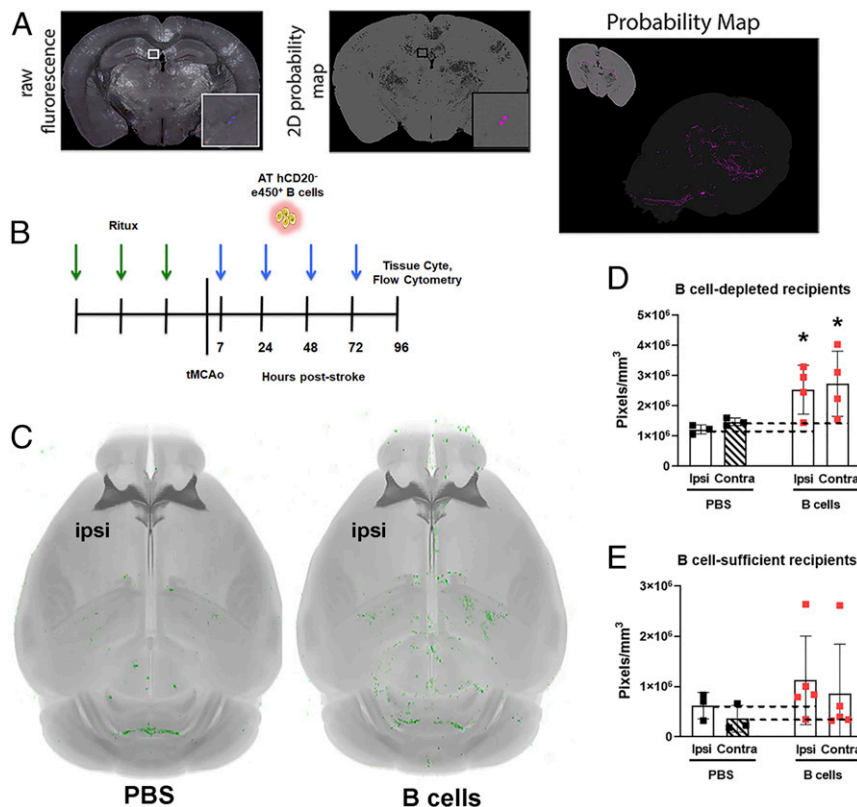


**Fig. 3.** Establishing whole-brain quantification of neuroinflammation using STPT. (A) Representative coronal section image acquired via STPT shown as a multichannel raw fluorescence merged image. (Magnification: *Left*, 16 $\times$ .) (*Inset*) e450<sup>+</sup> B cells present in the hippocampus (blue). (*Right*) Corresponding 2D probability map from the same coronal section in which the trained machine-learning algorithm classified pixels likely to represent brain parenchyma (gray) and e450<sup>+</sup> B cells (magenta). A 3D rendering of the B cell and parenchyma probability maps for each section in the whole brain are shown (*Right*). (B) Timeline for B cell depletion immediately prior to a transient middle cerebral artery occlusion (tMCAo), with adoptive transfer (AT) of e450<sup>+</sup> B cells. (C) Whole-brain images show a representative brain from the PBS- (*Left*) and B cell-treated (*Right*) cohorts. The probability maps of e450<sup>+</sup> B cells are shown in green and overlaid onto the average template from the atlas shown in grayscale. Ipsilesional (ipsi) hemisphere is identified. (D) Whole-hemisphere e450<sup>+</sup> fluorescence (in pixels per cubic millimeter) is shown for hCD20<sup>+</sup>-depleted mice that received PBS (black squares) or B cells (red squares). Dashed lines show mean PBS fluorescence that is used for normalization. (E) Similar to D, showing fluorescence in C57BL/6 mice that received PBS or B cells but without depletion of endogenous B cells. Significance determined by two-way ANOVA (\* $P < 0.05$  vs. respective PBS-treated control).

determine if B cells were infiltrating bilateral brain areas favorable to poststroke functional recovery. To achieve specific localization of neuroinflammation, raw fluorescent STPT images of every coronal section were registered with the corresponding sections in the CCFv3.0 atlas (Fig. 4A) in order to assess cellular e450<sup>+</sup> B cells across brain regions of interest (Fig. 4B). Quantification of e450-labeled B cells in whole-brain STPT datasets revealed brain regions with significant B cell diapedesis, including ipsilesional cerebral cortex, olfactory areas, and hypothalamus (Table 1). Contralateral areas with significant B cell diapedesis included olfactory areas, dentate gyrus, and hypothalamus, creating a bilateral diapedesis of B cells into brain regions typically spared in tMCAO-induced injury and that mediate motor and cognitive recovery, as well as active neurogenesis. To determine if endogenous B cells have an effect on adoptively transferred B

cells, we also adoptively transferred naive WT e450<sup>+</sup> B cells into poststroke WT mice that were not B cell-depleted. e450<sup>+</sup> donor B cells were again localized to the spleen and CLN after stroke (SI Appendix, Fig. S3E). STPT detected e450<sup>+</sup> B cells throughout the poststroke brain, even though e450<sup>+</sup> B cell signal was not significantly elevated over PBS controls due to more within-group fluorescent variation.

B cell diapedesis was elevated in five brain regions associated with motor function (i.e., cerebral cortex, cortical subplate, midbrain [sensory-related], cerebellum, and substantia nigra [reticular]) in B cell-depleted mice, which are highlighted in 3D surface renderings created by the Allen Institute for Brain Science Brain Explorer application (Fig. 4C). All areas demonstrated a similar magnitude of e450<sup>+</sup> B cell signal (100- to 200-fold higher than PBS fluorescence), with ipsilesional signals significant in

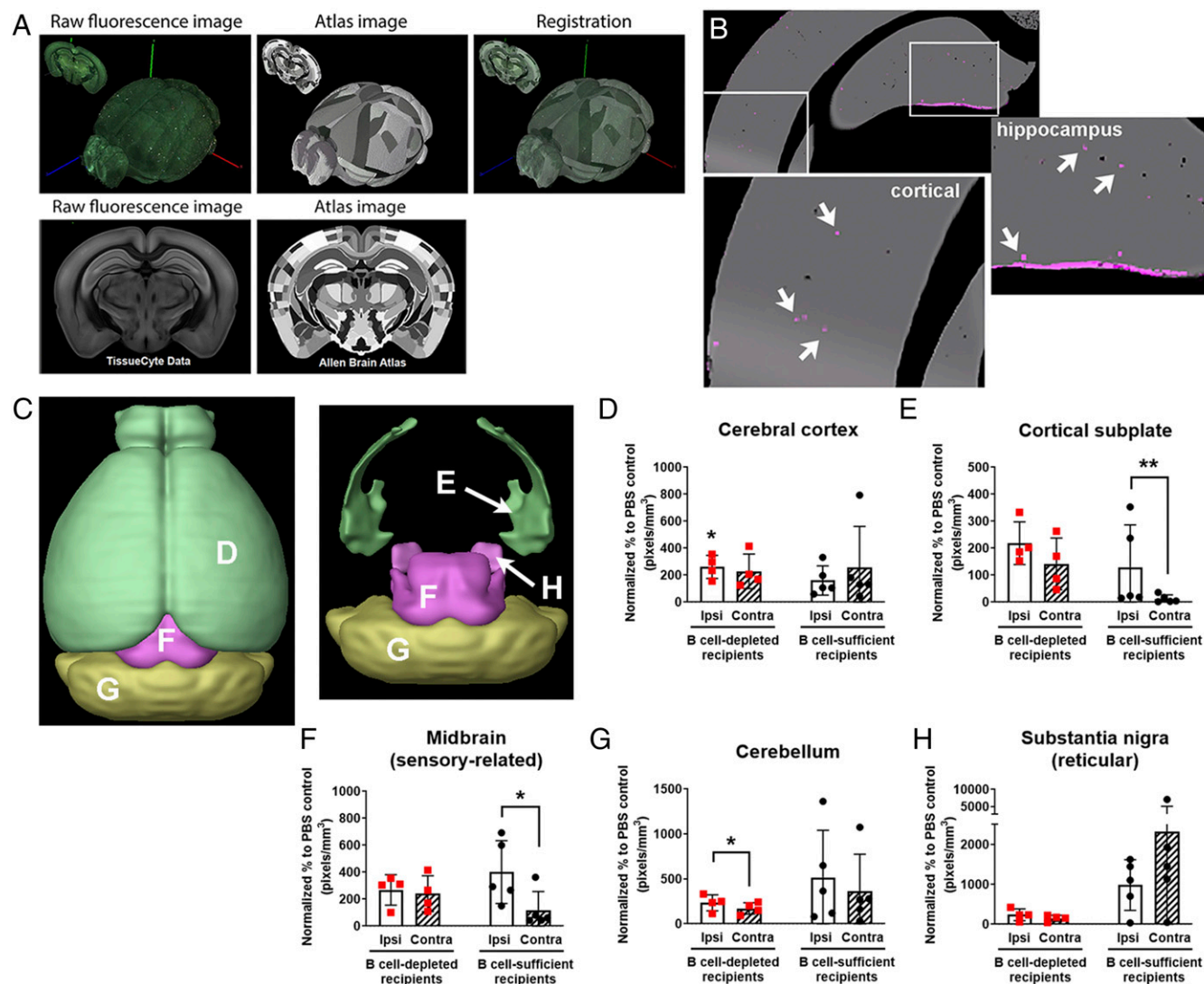


**Fig. 4.** B cells show diapedesis into remote motor areas after stroke. (A) Serial two-photon tomography images are coregistered to the Allen Institute CCF3.0 to allow identification of region-specific fluorescence in 3D whole-brain probability maps. (Magnification: A, 16 $\times$ .) (B) Representative areas classified as e450<sup>+</sup> B cells via machine learning (punctate magenta dots [*Insets*], identified by white arrows) that show B cell diapedesis in cortex and hippocampus (enlarged areas indicated by white squares). (C) Three-dimensional surface renderings created with the Brain Explorer application (Allen Institute for Brain Science) show regions with bilateral B cell diapedesis after stroke, with areas labeled to the letter corresponding to the data graphs. (D–H) Quantification of e450<sup>+</sup> B cell fluorescence in both B cell-depleted mice (red squares) and mice with endogenous B cells at time of stroke (black circles). Ipsilesional (ipsi, white bars) and contralateral (contra, hatched bars) brain regions show predominantly ipsilesional B cell diapedesis for (D) cerebral cortex, (E) cortical subplate, (F) midbrain, (G) cerebellum, and (H) substantia nigra with percent change (y-axis, pixels per cubic millimeter). Significance determined by paired *t* tests (\**P* < 0.05, \*\**P* < 0.01 vs. PBS controls unless indicated by brackets).

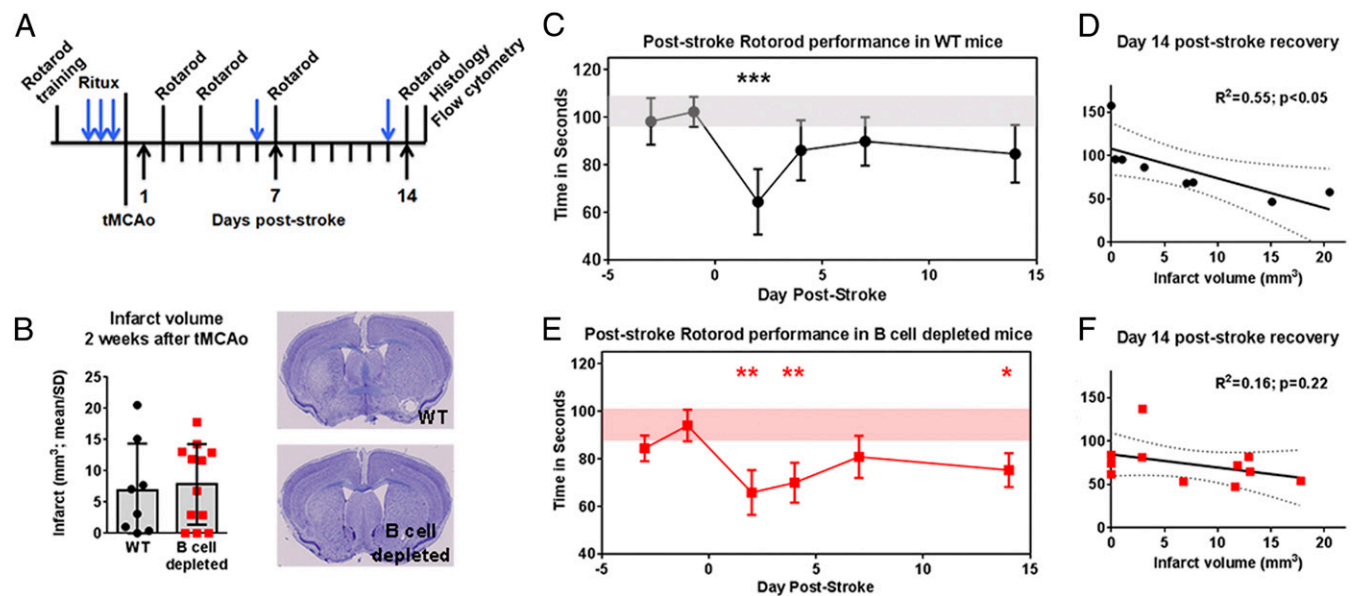
**Table 1. STPT data for e450<sup>+</sup> pixels for each brain region**

Brain region	Allen Brain Atlas abbreviation	Ipsilesional, mm <sup>3</sup>			Contralateral, mm <sup>3</sup>			Laterality index
		PBS control (n = 3)	B cells (n = 4)	P value	PBS control (n = 3)	B cells (n = 4)	P value	
<b>Gray matter</b>								
Cerebral cortex	CTX	8.6	22.44	<b>0.025*</b>	11.64	26.62	0.155	0.9
Olfactory areas	OLF	8.05	33.5	<b>0.019*</b>	10.1	32.46	<b>0.041*</b>	1.1
Dentate gyrus	DG	26.55	67.45	0.073	30.2	55	<b>0.028*</b>	1.2
Cerebral nuclei	CNU	4.25	10.62	<b>0.061</b>	8.09	18.78	0.202	0.7
Striatum	STR	3.88	9.27	<b>0.06</b>	8.16	18.34	0.227	0.6
Striatum ventral region	STRv	5.26	13.52	<b>0.06</b>	12.18	21.09	0.17	0.6
Cortical subplate	CTXsp	2.5	5.46	<b>0.066</b>	6.45	9.15	0.514	0.8
Hypothalamus	HY	11.85	32.21	<b>0.039*</b>	12.35	36.1	<b>0.020*</b>	0.9
Midbrain, sensory related	MBsen	28.09	75.47	<b>0.056</b>	35.38	85.27	0.136	0.9
Cerebellum	CB	10.32	24.14	<b>0.061</b>	12.96	22.32	0.128	1.1
<b>White matter</b>								
Corpus callosum	CC	1.29	4.41	0.313	1.98	6.44	0.242	0.8

STPT, serial two-photon tomography. Significance between PBS and B cell recipients per hemisphere was analyzed by unpaired, parametric. Student's *t* test: \**P* < 0.05; bolded text, *P* ≤ 0.06.

cerebral cortex (*P* < 0.05). Ipsilesional B cell diapedesis was also significantly higher compared to the contralateral hemisphere in the cerebellum (*P* < 0.05; Fig. 4G). In contrast, B cell-sufficient mice exhibited higher laterality for ipsilesional diapedesis, with more e450<sup>+</sup> B cell signal localized to the ipsilesional cortical subplate (*P* < 0.01; Fig. 4E) and midbrain (*P* < 0.05; Fig. 4F). Interestingly, one motor region, the substantia nigra pars reticulata, had much higher B cell diapedesis (1,000- to 2,000-fold vs. PBS) in the mice with endogenous B cells versus B cell-depleted mice (Fig. 4H), with highest values in the contralateral hemisphere. In summary, these data show that, in a mouse devoid of B cells, adoptively transferred B cells migrate to the motor areas to a similar magnitude in both the ipsi- and contralateral hemispheres, possibly exerting a supportive role in functional recovery.

**B Cells Contribute to Long-Term Motor Function Recovery.** As several motor areas remote from the tMCAo-mediated infarction exhibited B cell diapedesis, we hypothesized that long-term depletion of poststroke B cells could impede motor recovery. We tested this with prestroke depletion of B cells in hCD20<sup>+</sup> mice or WT hCD20<sup>-</sup> littermate controls receiving rituximab, with continuous depletion for 2 wk after tMCAo (Fig. 5A and SI Appendix, Fig. S4A). While an effect of B cell depletion on infarct volumes between cohorts (Fig. 5B) was observed, there was no genotype effect on motor skill acquisition during rotarod training (SI Appendix, Fig. S4B). WT mice exhibited a motor deficit at 2 d after tMCAo (*P* < 0.001; Fig. 5C) that recovered by 4 d relative to prestroke baseline. In contrast, B cell-depleted mice exhibited a significant loss in poststroke motor function at 2 d (*P* < 0.01;



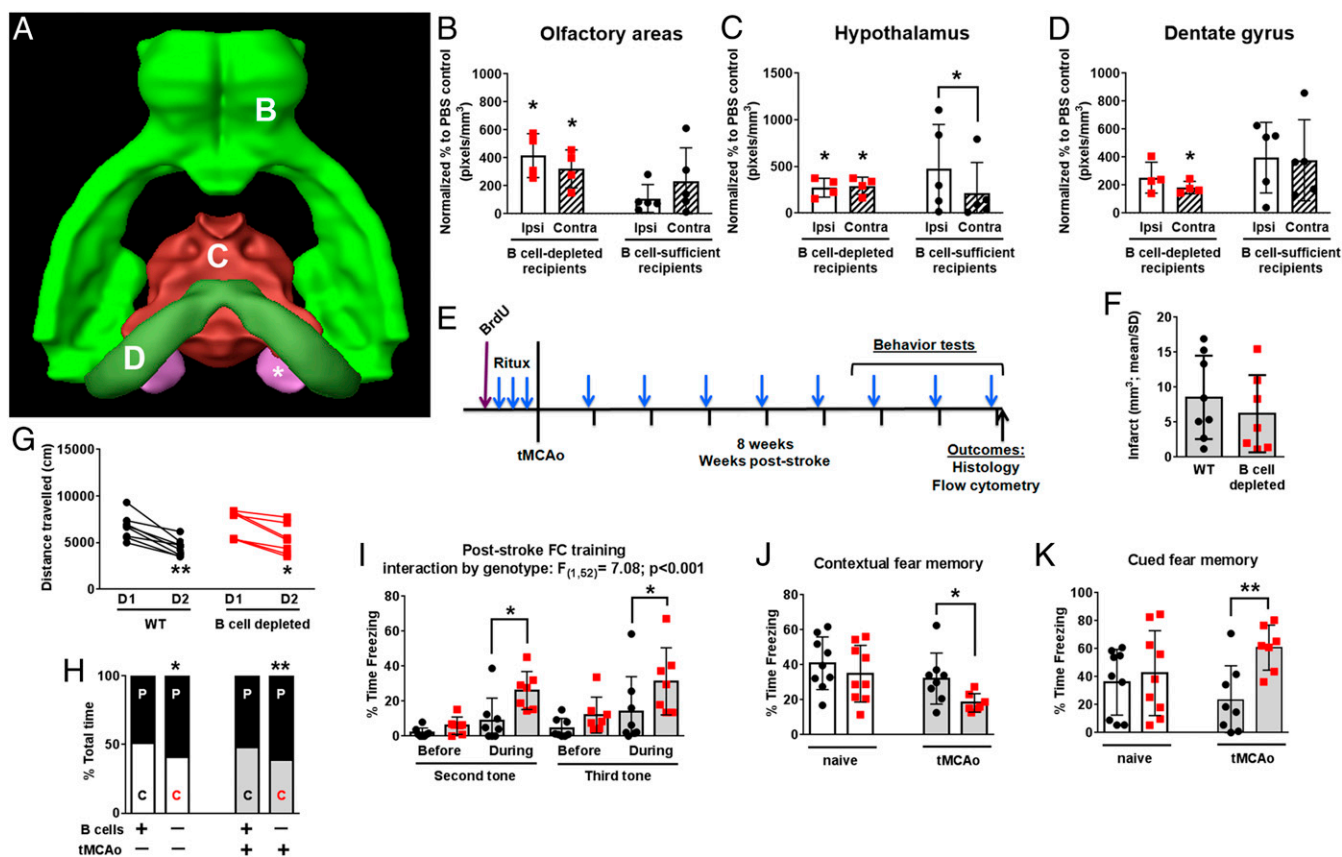
**Fig. 5. B cells support motor recovery after stroke.** (A) Experimental timeline for motor testing after transient middle cerebral artery occlusion (tMCAo). Rituximab treatment in wild type (WT; black circles) and B cell-depleted (red squares) mice show (B) infarct volumes that were similar between cohorts. Cresyl violet images for animals closest to the mean are shown. (Magnification: B, 20x, whole brain images.) (C) WT mice exhibited a motor deficit on a rotarod 2 d poststroke compared to prestroke baseline (horizontal gray bar) that (D) correlated to infarct volume. (E) B cell-depleted mice exhibited a loss in motor performance 2, 4, and 14 d poststroke compared to prestroke baseline (red horizontal bar), an observation (F) independent of infarct volume. Significance determined by Student's *t* test, one-way repeated-measure ANOVA, or linear correlation (\**P* < 0.05, \*\**P* < 0.01, \*\*\**P* < 0.001 vs. prestroke baseline). Dotted lines indicate 95% confidence interval.

Fig. 5E), 4 d ( $P < 0.01$ ), and 14 d ( $P < 0.05$ ) relative to prestroke baseline. There were no significant between-group differences. These data suggest that the absence of B cells after stroke could potentially impede plasticity in the motor network(s), located outside of the area of infarction, that support recovery of motor coordination. B cell depletion, however, did not affect the muscle strength, as analyzed by force grip analysis (*SI Appendix*, Fig. S4C). Infarct volumes only in WT mice negatively correlated with motor performance (Fig. 5D), with larger infarct volumes associated with poorer motor performance but lost with B cell depletion (Fig. 5F). With the observed bilateral B cell migration into brain regions associated with motor function, combined with the behavioral deficits in B cell-depleted mice, these data suggest that the presence of B cells may affect remote brain regions required for motor recovery (11).

**Poststroke B Cell Depletion Increases General Anxiety and Spatial Memory Deficits.** Initially, we observed significant e450<sup>+</sup> B cell signal in several brain regions (e.g., olfactory areas, dentate gyrus, substantia nigra, and hypothalamus) also associated with cognitive function (Fig. 6A) (31, 32). These areas, with the exception of the substantia nigra, show high bilateral e450<sup>+</sup> B cell signal. In the olfactory areas and the hypothalamus,

diapedesis of adoptively transferred B cells in B cell-depleted mice was significant ( $P < 0.05$ ) for both the ipsi- and contralesional hemispheres (both  $P < 0.05$  vs. PBS; Fig. 6B and C). The dentate gyrus is unique in that e450<sup>+</sup> B cell signal was significant in the contralesional hemisphere ( $P < 0.05$ ; Fig. 6D). Both the olfactory areas and the hypothalamus also exhibit increased signal in ipsi- vs. contralesional hemispheres, though the latter, surprisingly, is in the B cell-sufficient cohort. Thus, we sought to determine any associated poststroke cognitive deficits (e.g., locomotor activity, anxiety, learning, and memory) with B cell depletion extended through 8 wk after tMCAo (Fig. 6E). Interestingly, while rituximab maintained B cell depletion for 8 wk in both uninjured and tMCAo hCD20<sup>+</sup> cohorts (*SI Appendix*, Fig. S5A), WT poststroke mice also exhibited reductions in splenic B cell representation compared to uninjured WT mice ( $P < 0.05$ ).

As with the 2-wk motor recovery cohort shown in Fig. 5, there was no effect of long-term B cell depletion on infarct volumes (Fig. 6F). For the cognitive tests, we first measured locomotor activity using open field and found that the total distance traveled decreased between day 1 and day 2 for both poststroke WT ( $P < 0.01$ ) and B cell-depleted ( $P < 0.05$ ) cohorts (Fig. 6G).



**Fig. 6.** B cell depletion increases general anxiety and spatial memory deficits independent of infarct volume. (A) Brain Explorer surface rendering shows brain regions with B cell diapedesis related to cognitive function, including (B) olfactory areas, (C) hypothalamus, and (D) dentate gyrus, as indicated by letter in the figure. Both B cell-depleted mice (red squares) and mice with endogenous B cells at time of stroke (black circles) show B cell diapedesis in ipsilesional (ipsi, white bars) and contralesional (contra, hatched bars) brain regions. Fold change (y-axes) and significance vs. PBS controls shown unless indicated by brackets. (E) Experimental timeline for behavior testing in uninjured mice (white bars) or after transient middle cerebral artery occlusion (tMCAo; gray bars). (F) B cell depletion did not affect infarct volumes or (G) total movement in the open field. (H) Both uninjured and poststroke B cell-depleted mice spent more time in the periphery ("P") of the open field compared to the center ("C") of the field. (I) On the first day of cued and contextual fear-conditioning, poststroke B cell-depleted mice exhibited prolonged freezing during the training tones/shocks. (J) The next day, these same mice exhibited a worse spatial memory. (K) On the last day, B cell-depleted mice again exhibited more freezing during cued memory. Data graphed as mean  $\pm$  SD. Significance determined by paired *t* test, Student's *t* test, or repeated-measures ANOVA ( $*P < 0.05$ ,  $**P < 0.01$  vs. nondepleted control or D1 unless indicated by brackets).

Interestingly, though all cohorts traveled similar distances, B cell-depleted mice, regardless of injury, exhibited a preference to travel in the periphery of the open field compared to WT uninjured ( $P < 0.05$ ) or stroke-injured mice ( $P < 0.01$ ; Fig. 6H). Subsequent nonaversive cognitive assessment by novel object and novel location (33) failed to show differences between cohorts based on either genotype or stroke (SI Appendix, Fig. S5 C–F). Finally, we assessed hippocampal-dependent and -independent forms of learning and memory using a contextual and cued fear-conditioning paradigm, respectively. During the training phase, there was a significant effect of genotype for poststroke mice ( $P < 0.001$ ), as B cell-depleted mice froze for longer durations during the second, third (both  $P < 0.05$ ; Fig. 6I), and final ( $P < 0.05$ ; SI Appendix, Fig. S5G) tones. The next day, evaluation of contextual, hippocampal-dependent memory showed that B cell-depleted poststroke mice had worse recall compared to WT mice ( $P < 0.05$ ; Fig. 6J). In contrast, hippocampal-independent (i.e., amygdala-mediated) cued memory recall was exaggerated in B cell-depleted mice ( $P < 0.01$ ; Fig. 6K). These data suggest that long-term B cell depletion independently influences both hippocampal- and amygdala-dependent cognitive functions after stroke.

**B Cell Support of Poststroke Neurogenesis.** Adult neurogenesis occurs in the subventricular zone (SVZ) and the subgranular zone (SGZ) of the dentate gyrus, within the hippocampus (34). Stroke is also a potent inducer of neurogenesis (35, 36), although the mechanism is still poorly understood. Interestingly, of the 40 brain regions assessed for B cell migration in the poststroke brain, the two associated with neurogenesis were significant: olfactory areas, including the lateral olfactory tract, and the dentate gyrus (Fig. 6 B and D). In fact, a greater magnitude of e450<sup>+</sup> B cell signal over PBS controls occurred in the dentate gyrus of mice with endogenous B cell populations, again with an almost equivalent bilateral signal similar to the B cell-depleted cohort. These data demonstrate that B cells exhibit significant migration patterns into areas associated with neurogenesis yet outside of the ischemic injury. We thus quantified hippocampal neurogenesis 2 wk after tMCAo. Doublecortin-expressing (DCX<sup>+</sup>) cells are immature neuroblasts generated in the inner granular cell layer (GCL) of the hippocampal dentate gyrus (37), and DCX<sup>+</sup> cell bodies are an index of neurogenesis. Two weeks of B cell depletion

did not affect DCX<sup>+</sup> cell numbers (Fig. 7B) and GCL volume (SI Appendix, Fig. S6A) in otherwise healthy mice. Two weeks after tMCAo, however, WT mice had more DCX<sup>+</sup> neuroblasts in the dentate gyrus of the ipsilesional hemisphere compared to the contralesional hemisphere ( $P < 0.01$ ; Fig. 7C), consistent with other studies (35, 38). In contrast, the B cell-depleted mice did not exhibit increased poststroke neurogenesis ( $P < 0.001$  vs. WT). Changes (or lack thereof) in DCX<sup>+</sup> cell number were not associated with changes in GCL volume (Fig. 7D). In combination with the *in vivo* data (Fig. 6), these data suggest that B cells contribute to both stroke-induced neurogenesis and poststroke cognitive recovery, although removal of B cells does not affect basal (i.e., homeostatic) neurogenesis. Next, we quantified hippocampal cell survival via bromodeoxyuridine (BrdU) injection prior to the first rituximab treatment in the cognitive cohorts shown in Fig. 6. BrdU birthdates new neurons, and we determined long-term (i.e., 8 wk) cell survival in the hippocampus following continued poststroke B cell depletion. Basal cell survival in the uninjured mice was unaffected by long-term rituximab treatment (SI Appendix, Fig. S6B), similar to the DCX<sup>+</sup> population data. Stroke induced an increase in the ipsilateral BrdU<sup>+</sup> neurons of adult-generated hippocampal cells in the ischemic hemisphere of WT mice 8 wk after tMCAo ( $P < 0.05$  vs. contralesional hemisphere), but not B cell-depleted mice (Fig. 7E and F). As all mice received rituximab to control for off-target drug effects, this confirms a role for B cells in sustaining neuronal cell survival in areas outside of the ischemic injury.

## Discussion

Under physiological conditions, neuroplasticity occurs throughout life in cortical, subcortical, and cerebellar brain regions [e.g., olfactory areas (34), motor cortex (39, 40), hippocampus (34, 41), and cerebellum (42, 43)]. These areas are responsible for brain development, neurogenesis, learning, and memory formation. Following stroke, the spinal cord and brain, including the brain regions regulating motor and cognitive function, undergo significant neuroplasticity to reinnervate injured areas and reorganize neural networks supporting recovery (44–49). While neuroplasticity occurring within the ipsilesional hemisphere can improve functional outcome (46, 50–52), bihemispheric plasticity in the contralesional hemisphere also supports recovery (53–57).

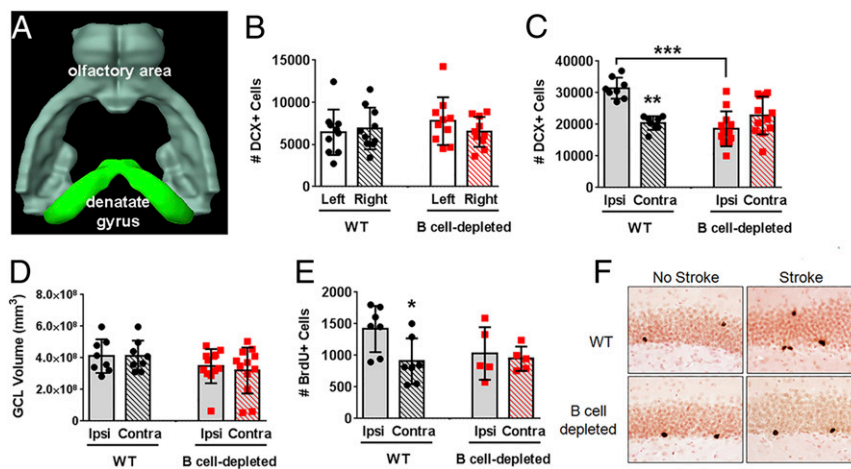


**Fig. 7.** B cells support poststroke neurogenesis. (A) Brain Explorer surface rendering shows neurogenic regions with bilateral B cell diapedesis after stroke. (B) B cell depletion did not alter basal neurogenesis in the dentate gyrus in the absence of stroke. (C) Stroke induced neurogenesis (i.e., doublecortin [DCX]<sup>+</sup> cells) in the ipsilesional (ipsi) hemisphere of wild type (WT; black circles) mice but not B cell-depleted (red squares) mice (D) independent of changes in granule cell layer (GCL) volume. (E) Stroke increased bromodeoxyuridine (BrdU)<sup>+</sup> cells in the dentate gyrus over contralesional (contra) numbers only in WT mice, (F) as shown by immunohistochemical detection of BrdU-positive cells, that was lost with long-term B cell depletion of healthy mice. Significance determined by one-way ANOVA (\* $P < 0.05$ ; \*\* $P < 0.01$ ; \*\*\* $P < 0.001$  vs. ipsilesional hemisphere unless indicated by brackets).



While our understanding of whole-brain neuroplasticity following stroke is ever-evolving, few studies investigate neuroinflammation in reorganizing brain regions. We previously found a high diapiesis of B cells into the poststroke brain, with a concomitant up-regulation of CXCL13 in cortical and subcortical brain areas (22, 23). Here, our advanced whole-brain imaging and analysis methods highlight significant bilateral migration of B cells to select brain regions, including the aforementioned regions undergoing poststroke plasticity, that are outside of the area of infarction and thus distant to the epicenter of poststroke neuroinflammation.

B cells are part of the adaptive immune system, and are responsible for many immunological functions, including antibody production, modulation of T cell responses, and antigen presentation (14). However, what is becoming increasingly apparent in animal studies of stroke is that not only the location, but also the timing and type, of B cell activation is critical in determining the contribution to stroke injury and/or repair (10, 21). B cells lack an acute (day 1 to 3 post stroke) physiological role in stroke pathology, indicating that their effector function is irrelevant to stroke etiology or innate immune modulation (20). B cells can produce several neurotrophins capable of supporting plasticity and neurogenesis, including brain-derived neurotrophic factor (BDNF) and nerve growth factor (NGF), in addition to IL-10 (15, 58, 59). Our *in vitro* data confirm a neurotrophic effect of B cells on the survival and health of neurons, as well as dendritic arborization, in mixed cortical cultures. Interestingly, treatment of mixed cortical cultures with IL-10-deficient B cells was not neuroprotective for total neuronal counts, but a 1:1 ratio of IL-10-deficient B cells to mixed cortical cells still protected arborization. This suggests that IL-10 is not the only neuroprotective effector produced by B cells following oxygen-glucose deprivation that should be addressed in future studies.

The neurotrophic effect of B cells is also reflected in our long-term hippocampal neurogenesis and cell survival data, wherein increases in both cellular processes require the active presence of B cells after stroke. The adult brain has the capacity to induce neurogenesis within the SGZ of the dentate gyrus and the SVZ of the lateral ventricle (60). Ischemic insult significantly increases neurogenesis in the SGZ and SVZ (61), with several studies also suggesting that neuroblasts migrate from the SVZ and SGZ to areas of ischemia, with the potential to adapt a neuronal phenotype and integrate into existing circuitry (35, 62). Others found that Copaxone (i.e., glatiramer acetate), which promotes the development of regulatory T (63) and B (Breg) cells (64, 65), induced both ipsi- and contralesional neurogenesis in a murine model of stroke concomitant with improved recovery (66), even though a specific B cell response was not investigated. However, we did not see an effect of B cell depletion on basal levels of neurogenesis or neuronal survival in otherwise healthy young mice. Other forms of neuroinflammation, particularly the microglial response (67), can modulate induction of poststroke neurogenesis. However, microglia do not play a role in the age-related decline of basal levels of neurogenesis in rats (68). Thus, future studies should investigate whether a natural, age-related decline in B cell lymphopoiesis, and thus declining circulating B cells and their neurotrophic capacity (69), contributes to lower basal neurogenesis with age. Of course, our study does not exclude other neuronal regeneration mechanisms, and future studies could use additional methods such as electrophysiology in order to more fully elucidate the neurotrophic function of B cells.

Our data suggest several future directions for study. While skilled motor rehabilitation improves motor function concomitant with neurogenesis (70), we used several additional cognitive tests to assess hippocampal-related recovery. Long-term B cell depletion increased anxiety with a concomitant decrease in contextual fear memory, suggesting both hippocampal and amygdala-related deficits, though these deficits were only present under stressful testing conditions and not during nonaversive testing.

Additional tests should augment our cognitive testing, especially in light of prior conflicting studies showing an active role of B cells in the development of poststroke cognitive decline in mice (21). We also previously identified that preconditioning down-regulated B cell antigen presentation and antibody production (22) and that poststroke B cell diapiesis in preconditioned mice correlated with fewer CD4 T cells and macrophages in the ipsilesional hemisphere (30). It was therefore understandably surprising to find that the adoptive transfer of this novel B cell subset did not reduce infarct volumes and, in fact, inhibited long-term motor recovery. B cell adoptive transfer into Rag<sup>-/-</sup> mice did not show evidence of poststroke neuroprotection either, indicating that B cell neuroprotection may be dependent on multiple lymphocyte subset synergism (18). It must be noted that our study used mature adult mice, and further understanding would necessitate the incorporation of female and aged (>18 mo) mice. This interaction with resident cells or, more intriguingly, the possibly detrimental inability of interaction from anergic B cells suggests a complicated poststroke immune response that potentially may be manipulated for a much longer window of time to induce neuroprotection.

Several clinical studies confirm a role for the B cell immune response in stroke, evident by the presence of immunoglobulins in the CSF of stroke patients (71–73) and the presence of antibody deposits in the brain of individuals with poststroke dementia (21). However, whether these are epiphenomena or represent an active role of B cells in neuropathology and/or functional recovery remains to be determined. Recovery occurs for months following stroke onset in patients, with better recovery associated with anatomical and functional plasticity (74, 75) and angiogenesis (76) in the ipsilesional hemisphere. Even though neuroplasticity occurs rapidly and robustly within an acute time window after stroke, neuroplasticity can last for years after stroke and support the long-term improvement of functional outcomes (11, 77). As stroke remains a leading cause of adult disability (1), it is vital to identify mechanisms that can contribute to neuroplasticity in neural networks. This includes new studies into long-term neuroinflammatory mechanisms that could be either detrimental or beneficial to stroke recovery depending on the timing of activation, the responding leukocyte subset, and now also the remote brain region(s) in which the responding immune cells migrate.

## Materials and Methods

**Mice.** All experiments used male mice that were 2 to 4 mo old at the start of experimentation and maintained in accordance to NIH guidelines for the care and use of laboratory animals. UT Southwestern Medical Center approved all procedures according to AAALAC accreditation and current PHS Animal Welfare Assurance requirements. Transgenic human CD20<sup>+</sup> expressing (hCD20<sup>+/+</sup>) mice were obtained from Mark Shlomchik (University of Pittsburgh, Pittsburgh, PA). C57BL/6J mice and B6.Cg-Tg(Thy1-YFP)16Jrs/J mice were purchased from Jackson Laboratory, and Swiss Webster mice were purchased from Harlan. Mice were group-housed in cages of 2 to 4 mice in standard animal housing with cob bedding, a 12/12-h light cycle with lights on at 6:00 AM, and food and water *ad libitum*. A total of 125 mice were used in experiments, with 84 undergoing tMCAo surgery. A total of 23 were excluded (73% success), including 6 for failure to meet blood flow criteria, 16 for death during or after surgery, and 1 for a lack of B cell depletion.

**B Cell Depletion and Repletion.** Rituximab (Micromedex) was given to hCD20<sup>+/+</sup> and hCD20<sup>-/-</sup> (littermate controls) at a standard dose of 100  $\mu$ g *i.p.* for three consecutive days before tMCAo (29). Each mouse was administered a weekly additional dose of rituximab thereafter to target the turnover of B cells. Successful and sustained B cell depletion was confirmed by isolating lymphocytes from spleen 2 or 8 wk post tMCAo that were stained with a general antibody panel and quantified by flow cytometry (78–80). B cells were purified from the splenocyte population using magnetic bead separation (Stem Cell Technologies). Purity was verified by flow cytometry. A total of  $5 \times 10^6$  B cells were transferred *i.v.* in 0.2 mL 0.1 M PBS. B cells for imaging were labeled with eFluor 450 (e450) proliferation dye (eBioscience 65–0842-85). Hemocytometer counts were not collected for one cohort of B

cell-depleted mice in the long-term cognitive studies, so percent representation of CD45<sup>+</sup> cells is shown *SI Appendix, Fig. S4A*.

**Statistical Analysis.** Power analysis based on previous results and published data determined the approximate number of animals given an expected 30% stroke-induced mortality rate (80). Statistical differences were analyzed using unpaired parametric two-sample Student's *t* test, ratio paired Student's *t* test, one-way repeated-measures ANOVA, or two-way ANOVA where appropriate and as indicated in the text (Graph Pad Prism 6.0). Values of *P* < 0.05 were considered significant. All experimenters were blinded to condition, and all animals were randomly assigned to group.

All detailed protocols for tMCAo induction, imaging (Tissuecyte, MRI), histology, stereology, flow cytometry, motor and cognitive assays, and in vitro culture assays are available in *SI Appendix, Methods*.

**Data Availability Statement.** All data discussed in the paper are available to readers through Harvard Dataverse, <https://doi.org/10.7910/DVN/RFGT4S>.

1. A. S. Go *et al.*; American Heart Association Statistics Committee and Stroke Statistics Subcommittee, Executive summary: Heart disease and stroke statistics—2014 update: A report from the American Heart Association. *Circulation* **129**, 399–410 (2014).
2. Á. Chamorro *et al.*, The immunology of acute stroke. *Nat. Rev. Neurol.* **8**, 401–410 (2012).
3. M. Gelderblom *et al.*, Temporal and spatial dynamics of cerebral immune cell accumulation in stroke. *Stroke* **40**, 1849–1857 (2009).
4. J. T. Walsh *et al.*, MHCII-independent CD4<sup>+</sup> T cells protect injured CNS neurons via IL-4. *J. Clin. Invest.* **125**, 2547 (2015).
5. J. Wang *et al.*, Activated regulatory T cell regulates neural stem cell proliferation in the subventricular zone of normal and ischemic mouse brain through interleukin 10. *Front. Cell. Neurosci.* **9**, 361 (2015).
6. A. Liesz *et al.*, Inhibition of lymphocyte trafficking shields the brain against deleterious neuroinflammation after stroke. *Brain* **134**, 704–720 (2011).
7. T. Shichita *et al.*, Pivotal role of cerebral interleukin-17-producing gammadelta T cells in the delayed phase of ischemic brain injury. *Nat. Med.* **15**, 946–950 (2009).
8. K. J. Becker, P. Tanzi, D. Zierath, M. S. Buckwalter, Antibodies to myelin basic protein are associated with cognitive decline after stroke. *J. Neuroimmunol.* **295–296**, 9–11 (2016).
9. S. Bodhankar, Y. Chen, A. A. Vandenbark, S. J. Murphy, H. Offner, IL-10-producing B-cells limit CNS inflammation and infarct volume in experimental stroke. *Metab. Brain Dis.* **28**, 375–386 (2013).
10. S. Bodhankar, Y. Chen, A. A. Vandenbark, S. J. Murphy, H. Offner, Treatment of experimental stroke with IL-10-producing B-cells reduces infarct size and peripheral and CNS inflammation in wild-type B-cell-sufficient mice. *Metab. Brain Dis.* **29**, 59–73 (2014).
11. N. Dancause, R. J. Nudo, Shaping plasticity to enhance recovery after injury. *Prog. Brain Res.* **192**, 273–295 (2011).
12. E. T. Urban, 3rd *et al.*, Gene expression changes of interconnected spared cortical neurons 7 days after ischemic infarct of the primary motor cortex in the rat. *Mol. Cell. Biochem.* **369**, 267–286 (2012).
13. A. M. Stowe *et al.*, VEGF protein associates to neurons in remote regions following cortical infarct. *J. Cereb. Blood Flow Metab.* **27**, 76–85 (2007).
14. U. M. Selvaraj, K. Poinsatte, V. Torres, S. B. Ortega, A. M. Stowe, Heterogeneity of B cell functions in stroke-related risk, prevention, injury, and repair. *Neurotherapeutics* **13**, 729–747 (2016).
15. A. L. Fauchais *et al.*, Role of endogenous brain-derived neurotrophic factor and sortilin in B cell survival. *J. Immunol.* **181**, 3027–3038 (2008).
16. R. Tabakman, S. Lecht, S. Sephanova, H. Arien-Zakay, P. Lazarovici, Interactions between the cells of the immune and nervous system: Neurotrophins as neuroprotection mediators in CNS injury. *Prog. Brain Res.* **146**, 387–401 (2004).
17. X. Ren *et al.*, Regulatory B cells limit CNS inflammation and neurologic deficits in murine experimental stroke. *J. Neurosci.* **31**, 8556–8563 (2011).
18. G. Yilmaz, T. V. Arumugam, K. Y. Stokes, D. N. Granger, Role of T lymphocytes and interferon-gamma in ischemic stroke. *Circulation* **113**, 2105–2112 (2006).
19. C. Kleinschnitz *et al.*, Early detrimental T-cell effects in experimental cerebral ischemia are neither related to adaptive immunity nor thrombus formation. *Blood* **115**, 3835–3842 (2010).
20. M. K. Schuhmann, F. Langhauser, P. Kraft, C. Kleinschnitz, B cells do not have a major pathophysiologic role in acute ischemic stroke in mice. *J. Neuroinflammation* **14**, 112 (2017).
21. K. P. Doyle *et al.*, B-lymphocyte-mediated delayed cognitive impairment following stroke. *J. Neurosci.* **35**, 2133–2145 (2015).
22. N. L. Monson *et al.*, Repetitive hypoxic preconditioning induces an immunosuppressed B cell phenotype during endogenous protection from stroke. *J. Neuroinflammation* **11**, 22 (2014).
23. U. M. Selvaraj *et al.*, Preconditioning-induced CXCL12 upregulation minimizes leukocyte infiltration after stroke in ischemia-tolerant mice. *J. Cereb. Blood Flow Metab.* **37**, 801–813 (2017).
24. T. Ragan *et al.*, Serial two-photon tomography for automated ex vivo mouse brain imaging. *Nat. Methods* **9**, 255–258 (2012).

**ACKNOWLEDGMENTS.** The authors acknowledge Drs. Abhijit Budge, Shanrong Zhang, and Shari Birnbaum for their technical expertise for imaging and behavioral analyses and data acquisition. The authors also acknowledge UT Southwestern's Flow Cytometry Core, the Moody Foundation Flow Cytometry Facility at the Children's Research Institution, the Advanced Imaging Research Center (Shared Instrumental Grant NIH15100D023552-01), Rodent Behavior Core Facility, the Whole Brain Microscopy Facility, and the Neuro-Models Facility with Laura Ingle. This study was funded by grants to A.M.S. from the American Heart Association (14SDG18410020), NIH/NINDS (NS088555), the Dana Foundation David Mahoney Neuroimaging Program, and The Haggerty Center for Brain Injury and Repair (UTSW); to S.B.O. from the American Heart Association (14POST20480373) and NIH/NINDS (3R01NS088555-03S1); to V.O.T. from the NIH/NIAID (5T32AI005284-40) and NIH/NINDS (3R01NS088555-02S1); to U.M.S. from the American Heart Association (17PRE33660147); and to A.J.E. from the NIH (DA023701, DA023555, MH107945) and the US National Aeronautics and Space Administration (NNX15AE09G). S.E.L. and C.W.V.W. were funded by an NIH institutional training grant (DA007290, Basic Science Training Program in the Drug Abuse Research, Principal Investigator A.J.E.). The UT Southwestern Whole Brain Microscopy Facility and the Neuro-Models Facility are supported by the Texas Institute for Brain Injury and Repair (TIBIR).

25. Y. Kim *et al.*, Mapping social behavior-induced brain activation at cellular resolution in the mouse. *Cell Rep.* **10**, 292–305 (2015).
26. D. A. Vouden *et al.*, Whole-brain mapping of behaviourally induced neural activation in mice. *Brain Struct. Funct.* **220**, 2043–2057 (2015).
27. K. Poinsatte *et al.*, Visualization and quantification of post-stroke neural connectivity and neuroinflammation using serial two-photon tomography in the whole mouse brain. *Front. Neurosci.* **13**, 1055 (2019).
28. D. M. O. Ramirez, D. A. Ajay, M. P. Goldberg, J. P. Meeks, *Serial Multiphoton Tomography and Analysis of Volumetric Images of the Mouse Brain. Multiphoton Microscopy, Neuromethods series* (Springer Nature, 2019).
29. N. L. Monson *et al.*, Rituximab therapy reduces organ-specific T cell responses and ameliorates experimental autoimmune encephalomyelitis. *PLoS One* **6**, e17103 (2011).
30. U. M. Selvaraj *et al.*, Preconditioning-induced CXCL12 upregulation minimizes leukocyte infiltration after stroke in ischemia-tolerant mice. *J. Cereb. Blood Flow Metab.* (Nihongban) **37**, 801–813 (2017).
31. E. R. Duval, A. Javanbakht, I. Liberzon, Neural circuits in anxiety and stress disorders: A focused review. *Ther. Clin. Risk Manag.* **11**, 115–126 (2015).
32. L. M. Shin, I. Liberzon, The neurocircuitry of fear, stress, and anxiety disorders. *Neuropsychopharmacology* **35**, 169–191 (2010).
33. K. O. Cho *et al.*, Aberrant hippocampal neurogenesis contributes to epilepsy and associated cognitive decline. *Nat. Commun.* **6**, 6606 (2015).
34. G. L. Ming, H. Song, Adult neurogenesis in the mammalian brain: Significant answers and significant questions. *Neuron* **70**, 687–702 (2011).
35. W. Jiang, W. Gu, T. Brännström, R. Rosqvist, P. Wester, Cortical neurogenesis in adult rats after transient middle cerebral artery occlusion. *Stroke* **32**, 1201–1207 (2001).
36. J. M. Parent, Z. S. Vexler, C. Gong, N. Derugin, D. M. Ferriero, Rat forebrain neurogenesis and striatal neuron replacement after focal stroke. *Ann. Neurol.* **52**, 802–813 (2002).
37. G. Kempermann, S. Jessberger, B. Steiner, G. Kronenberg, Milestones of neuronal development in the adult hippocampus. *Trends Neurosci.* **27**, 447–452 (2004).
38. E. Gould, B. S. McEwen, P. Tanapat, L. A. Galea, E. Fuchs, Neurogenesis in the dentate gyrus of the adult tree shrew is regulated by psychosocial stress and NMDA receptor activation. *J. Neurosci.* **17**, 2492–2498 (1997).
39. J. N. Sanes, J. P. Donoghue, Plasticity and primary motor cortex. *Annu. Rev. Neurosci.* **23**, 393–415 (2000).
40. T. A. Clark, M. Fu, A. K. Dunn, Y. Zuo, T. A. Jones, Preferential stabilization of newly formed dendritic spines in motor cortex during manual skill learning predicts performance gains, but not memory endurance. *Neurobiol. Learn. Mem.* **152**, 50–60 (2018).
41. Y. Gu, S. Janoschka, S. Ge, Neurogenesis and hippocampal plasticity in adult brain. *Curr. Top. Behav. Neurosci.* **15**, 31–48 (2013).
42. J. Carrillo, S. Y. Cheng, K. W. Ko, T. A. Jones, H. Nishiyama, The long-term structural plasticity of cerebellar parallel fiber axons and its modulation by motor learning. *J. Neurosci.* **33**, 8301–8307 (2013).
43. E. D'Angelo, The organization of plasticity in the cerebellar cortex: From synapses to control. *Prog. Brain Res.* **210**, 31–58 (2014).
44. D. L. Adkins, J. E. Hsu, T. A. Jones, Motor cortical stimulation promotes synaptic plasticity and behavioral improvements following sensorimotor cortex lesions. *Exp. Neurol.* **212**, 14–28 (2008).
45. L. I. Benowitz, S. T. Carmichael, Promoting axonal rewiring to improve outcome after stroke. *Neurobiol. Dis.* **37**, 259–266 (2010).
46. J. Biernaskie, A. Szymanska, V. Windle, D. Corbett, Bi-hemispheric contribution to functional motor recovery of the affected forelimb following focal ischemic brain injury in rats. *Eur. J. Neurosci.* **21**, 989–999 (2005).
47. J. D. Riley *et al.*, Anatomy of stroke injury predicts gains from therapy. *Stroke* **42**, 421–426 (2011).
48. J. V. Perederiy, G. L. Westbrook, Structural plasticity in the dentate gyrus—revisiting a classic injury model. *Front. Neural Circuits* **7**, 17 (2013).
49. A. R. Luft *et al.*, Brain activation of lower extremity movement in chronically impaired stroke survivors. *Neuroimage* **26**, 184–194 (2005).

50. M. L. Starkey *et al.*, Back seat driving: Hindlimb corticospinal neurons assume forelimb control following ischaemic stroke. *Brain* **135**, 3265–3281 (2012).
51. L. Wang, J. M. Conner, A. H. Nagahara, M. H. Tuszynski, Rehabilitation drives enhancement of neuronal structure in functionally relevant neuronal subsets. *Proc. Natl. Acad. Sci. U.S.A.* **113**, 2750–2755 (2016).
52. T. A. Jones, D. L. Adkins, Motor system reorganization after stroke: Stimulating and training toward perfection. *Physiology (Bethesda)* **30**, 358–370 (2015).
53. N. T. Lindau *et al.*, Rewiring of the corticospinal tract in the adult rat after unilateral stroke and anti-Nogo-A therapy. *Brain* **137**, 739–756 (2014).
54. J. E. Hsu, T. A. Jones, Contralateral neural plasticity and functional changes in the less-affected forelimb after large and small cortical infarcts in rats. *Exp. Neurol.* **201**, 479–494 (2006).
55. C. M. Lapash Daniels, K. L. Ayers, A. M. Finley, J. P. Culver, M. P. Goldberg, Axon sprouting in adult mouse spinal cord after motor cortex stroke. *Neurosci. Lett.* **450**, 191–195 (2009).
56. Z. Liu, R. L. Zhang, Y. Li, Y. Cui, M. Chopp, Remodeling of the corticospinal innervation and spontaneous behavioral recovery after ischemic stroke in adult mice. *Stroke* **40**, 2546–2551 (2009).
57. T. H. McNeill, S. A. Brown, E. Hogg, H. W. Cheng, C. K. Meshul, Synapse replacement in the striatum of the adult rat following unilateral cortex ablation. *J. Comp. Neurol.* **467**, 32–43 (2003).
58. A. E. Edling, T. Nanavati, J. M. Johnson, V. K. Tuohy, Human and murine lymphocyte neurotrophin expression is confined to B cells. *J. Neurosci. Res.* **77**, 709–717 (2004).
59. T. Kiyota *et al.*, AAV serotype 2/1-mediated gene delivery of anti-inflammatory interleukin-10 enhances neurogenesis and cognitive function in APP+PS1 mice. *Gene Ther.* **19**, 724–733 (2012).
60. X. Duan, E. Kang, C. Y. Liu, G. L. Ming, H. Song, Development of neural stem cell in the adult brain. *Curr. Opin. Neurobiol.* **18**, 108–115 (2008).
61. K. Jin *et al.*, Neurogenesis in dentate subgranular zone and rostral subventricular zone after focal cerebral ischemia in the rat. *Proc. Natl. Acad. Sci. U.S.A.* **98**, 4710–4715 (2001).
62. A. Arvidsson, Z. Kokaia, O. Lindvall, N-methyl-D-aspartate receptor-mediated increase of neurogenesis in adult rat dentate gyrus following stroke. *Eur. J. Neurosci.* **14**, 10–18 (2001).
63. D. K. Tennakoon *et al.*, Therapeutic induction of regulatory, cytotoxic CD8+ T cells in multiple sclerosis. *J. Immunol.* **176**, 7119–7129 (2006).
64. P. H. Lalive *et al.*, Glatiramer acetate in the treatment of multiple sclerosis: Emerging concepts regarding its mechanism of action. *CNS Drugs* **25**, 401–414 (2011).
65. P. Putheti, M. Soderstrom, H. Link, Y. M. Huang, Effect of glatiramer acetate (Copaxone) on CD4+CD25high T regulatory cells and their IL-10 production in multiple sclerosis. *J. Neuroimmunol.* **144**, 125–131 (2003).
66. Y. Cruz *et al.*, Copolymer-1 promotes neurogenesis and improves functional recovery after acute ischemic stroke in rats. *PLoS One* **10**, e0121854 (2015).
67. M. K. Tobin *et al.*, Neurogenesis and inflammation after ischemic stroke: What is known and where we go from here. *J. Cereb. Blood Flow Metab.* **34**, 1573–1584 (2014).
68. V. Darsalia, U. Heldmann, O. Lindvall, Z. Kokaia, Stroke-induced neurogenesis in aged brain. *Stroke* **36**, 1790–1795 (2005).
69. Z. Keren *et al.*, B-cell depletion reactivates B lymphopoiesis in the BM and rejuvenates the B lineage in aging. *Blood* **117**, 3104–3112 (2011).
70. F. Wurm, S. Keiner, A. Kunze, O. W. Witte, C. Redecker, Effects of skilled forelimb training on hippocampal neurogenesis and spatial learning after focal cortical infarcts in the adult rat brain. *Stroke* **38**, 2833–2840 (2007).
71. H. Prüss *et al.*, Evidence of intrathecal immunoglobulin synthesis in stroke: A cohort study. *Arch. Neurol.* **69**, 714–717 (2012).
72. B. Roström, B. Link, Oligoclonal immunoglobulins in cerebrospinal fluid in acute cerebrovascular disease. *Neurology* **31**, 590–596 (1981).
73. S. A. Tsementzis, S. W. Chao, E. R. Hitchcock, J. S. Gill, D. G. Beevers, Oligoclonal immunoglobulin G in acute subarachnoid hemorrhage and stroke. *Neurology* **36**, 395–397 (1986).
74. K. R. Crafton, A. N. Mark, S. C. Cramer, Improved understanding of cortical injury by incorporating measures of functional anatomy. *Brain* **126**, 1650–1659 (2003).
75. C. Braun *et al.*, Crossed cortico-spinal motor control after capsular stroke. *Eur. J. Neurosci.* **25**, 2935–2945 (2007).
76. J. Krupinski, J. Kaluza, P. Kumar, S. Kumar, J. M. Wang, Role of angiogenesis in patients with cerebral ischemic stroke. *Stroke* **25**, 1794–1798 (1994).
77. P. W. Duncan, L. B. Goldstein, D. Matchar, G. W. Divine, J. Feussner, Measurement of motor recovery after stroke. Outcome assessment and sample size requirements. *Stroke* **23**, 1084–1089 (1992).
78. S. B. Ortega *et al.*, Stroke induces a rapid adaptive autoimmune response to novel neuronal antigens. *Discov. Med.* **19**, 381–392 (2015).
79. U. M. Selvaraj *et al.*, Selective nonnuclear estrogen receptor activation decreases stroke severity and promotes functional recovery in female mice. *Endocrinology* **159**, 3848–3859 (2018).
80. C. Lane-Donovan *et al.*, Physiologic Reelin does not play a strong role in protection against acute stroke. *J. Cereb. Blood Flow Metab.* **36**, 1295–1303 (2016).